



ARTICLE

Cellular and Molecular Biology

Diagnostic value of ¹⁸F-FDG-PET to predict the tumour immune status defined by tumoural PD-L1 and CD8⁺ tumour-infiltrating lymphocytes in oral squamous cell carcinoma

Maria Togo¹, Takehiko Yokobori², Kimihiro Shimizu³, Tadashi Handa¹, Kyoichi Kaira⁴, Takaaki Sano¹, Mariko Tsukagoshi², Tetsuya Higuchi⁵, Satoshi Yokoo⁶, Ken Shirabe³ and Tetsunari Oyama¹

BACKGROUND: Lately, immune checkpoint proteins, such as programmed death 1 (PD-1) and its ligand-1 (PD-L1), have garnered attention as a new target in oral squamous cell carcinoma (OSCC). Reportedly, fluoro-D-glucose (FDG)-uptake alteration by anti-PD-1 antibody treatment depicts the response in patients with lung cancer. This study aims to elucidate the correlations between tumour immune status, clinicopathological factors, ¹⁸F-FDG-uptake and cold tumour phenotypes as low PD-L1 expression/low CD8⁺ tumour-infiltrating lymphocytes (TILs) in OSCC.

METHODS: We performed immunohistochemical analysis of PD-L1, hypoxia-inducible factor 1 A (HIF-1A), glucose transporter type 1 (GLUT1), CD8, E-cadherin and Ki-67 on 59 operable OSCC samples. We assessed the correlations between these factors and preoperative ¹⁸F-FDG-uptake, clinicopathological characteristics and prognosis.

RESULTS: Low expression of PD-L1 in OSCC correlated with cancer aggressiveness, poor prognosis, high ¹⁸F-FDG-uptake with HIF-1A/GLUT1 and low E-cadherin expression and low CD8. Cold tumour phenotypes as low PD-L1 tumour cells and low stromal CD8 correlated with the poor prognosis, high ¹⁸F-FDG-uptake and E-cadherin suppression. Furthermore, the high level of preoperative ¹⁸F-FDG-uptake in OSCC was an independent predictor of the cold tumour immune status.

CONCLUSIONS: ¹⁸F-FDG-uptake is an independent predictor of cold tumour in OSCC. ¹⁸F-FDG-PET imaging could be a promising diagnostic tool to estimate tumour immune status.

British Journal of Cancer (2020) 122:1686–1694; <https://doi.org/10.1038/s41416-020-0820-z>

BACKGROUND

Although chemotherapy and radiotherapy may confer survival and organ preservation benefits in oral squamous cell carcinoma (OSCC),^{1,2} patients with therapeutic-resistant OSCC exhibit poor prognoses.³ Thus, further research is warranted worldwide to recognise new therapeutic targets and enhance the prognosis of patients with resistant OSCC.

Lately, immune checkpoint inhibitors (ICIs) have garnered considerable attention as a new innovative cancer therapy.^{4,5} Studies have demonstrated that targeting immune checkpoint proteins such as programmed death 1 (PD-1) and its ligand-1 (PD-L1) exerts a continuous and significant clinical effect and exhibits low toxicity in some responder patients with various cancer types.^{6–10} Conversely, almost all non-responding patients with cancer have been reported to gain no adequate benefits despite using ICIs.¹¹ Thus, presently, several researchers are focusing on the development of useful biomarkers to estimate the sensitivity of ICIs for patients with cancer. In fact, some studies have reported tumour immune status on the basis of

PD-L1-positive tumour cells/stromal CD8⁺ tumour-infiltrating lymphocytes (TILs), tumour mutation burden and interferon-γ gene signature as promising biomarker candidates for estimating sensitivity to ICIs.^{12–14} Among them, the tumour immune status of tumours with low PD-L1 expression/low activated tumour-specific CD8⁺TILs has been termed ‘cold tumour’, which correlates with poor local immune response and ICIs resistance when compared with the ICIs-sensitive hot tumour with high PD-L1 expression/high CD8⁺TILs.^{15,16} Reportedly, patients with OSCC correlate with suppressed tumour immunoreactivity and high levels of tumour mutation burden, which is associated with a good response to ICIs.^{17,18} Cold tumour has attracted attention as ICIs resistant marker, as well as being one of the therapeutic targets to improve the sensitivity of ICIs; however, the importance of cold tumour in patients with OSCC has not been previously reported. Nevertheless, invasive tumour sampling is essential in order to ascertain tumour immune status, including cold tumour phenotypes, DNA status and gene expression signature in tumour tissues.

¹Department of Diagnostic Pathology, Gunma University Graduate School of Medicine, Maebashi, Gunma, Japan; ²Department of Innovative Cancer Immunotherapy, Gunma University, Maebashi, Gunma, Japan; ³Department of General Surgical Science, Graduate School of Medicine, Gunma University, Maebashi, Gunma, Japan; ⁴Department of Respiratory Medicine, Comprehensive Cancer Center, International Medical Center, Saitama Medical University, Hidaka, Saitama, Japan; ⁵Department of Diagnostic Radiology and Nuclear Medicine, Gunma University, Maebashi, Gunma, Japan and ⁶Department of Oral and Maxillofacial Surgery and Plastic Surgery, Gunma University Graduate School of Medicine, Maebashi, Gunma, Japan

Correspondence: Maria Togo (m1620030@gunma-u.ac.jp) or Takehiko Yokobori (bori45@gunma-u.ac.jp)

Received: 14 June 2019 Revised: 24 January 2020 Accepted: 9 March 2020

Published online: 2 April 2020

Although the use of 2-deoxy-2-[fluorine-18]fluoro-D-glucose with positron emission tomography/computed tomography (¹⁸F-FDG-PET/CT) has been considered to be a non-invasive diagnostic tool in order to differentiate between cancer tissue and benign lesions, false-positive findings, such as high ¹⁸F-FDG-uptake, might occur in inflammatory diseases.¹⁹ Previously, we reported that the change in ¹⁸F-FDG-uptake before and after anti-PD-1 antibody nivolumab treatment signified the subtle nivolumab response in patients with lung cancer.²⁰ These findings indicated the possible correlation between ¹⁸F-FDG-uptake and the existing ICIs sensitivity markers, such as cold or hot tumour immune status, regarding the PD-L1 and CD8⁺TILs in tumour tissues. In addition, the tumoural PD-L1 expression has been reported to be associated with ¹⁸F-FDG-uptake in lung and bladder cancers,^{20,21} and hypoxia-inducible factor 1A (HIF-1A)/glucose transporter type 1 (GLUT1) signalling has been shown to be related to ¹⁸F-FDG-uptake.²² Furthermore, there are also reports on the relationship between epithelial-mesenchymal transition (EMT) and ¹⁸F-FDG-uptake.²³

However, to date, information regarding the clinicopathological significance, tumour immune status and the non-invasive assessment of ¹⁸F-FDG-uptake, which was regulated by the accumulation of HIF-1A and GLUT1 and EMT induction characterised by the epithelial marker suppression in OSCC, remains limited. Remarkably, the HIF-1A/GLUT1/EMT axis correlates with not only the cold tumour immune status but also chemoradiation therapy, cancer aggressiveness and poor prognosis.^{24–26}

This study aims to elucidate the correlation between tumour immune status, such as PD-L1-positive tumour cells/stromal CD8⁺TILs, and HIF-1A/GLUT1/EMT expression regarding the ¹⁸F-FDG-uptake in OSCC.

METHODS

Patient background

We enrolled patients with OSCC ($n = 59$; 28 males and 31 females) who underwent surgical resection at the Department of Oral and Maxillofacial Surgery, Gunma University Hospital (Maebashi, Gunma, Japan), from January 2009 to March 2014. Of note, no patient underwent chemotherapy or radiotherapy preoperatively. Of 59 patients, 50 received ¹⁸F-FDG-PET for preoperative assessment. In addition, the tumour staging was based on the Union for International Cancer Control Tumour-Node-Metastasis classification (seventh edition), General Rules for Clinical Studies on Head and Neck Cancer (fifth edition) and the mode of invasion (Y–K classification).²⁷ This study conformed to the tenets of the Helsinki Declaration and was approved by the Institutional Review Board for Clinical Research at the Gunma University Hospital (Maebashi, Gunma, Japan; approval number: 2018212). Patients' agreement was obtained with the opt-out method.

Immunohistochemistry

We cut a 4- μ m section from paraffin blocks of samples, thereafter mounting each section on a silane-coated glass slide, deparaffinising and soaking for 30 min at room temperature in 0.3% H₂O₂/methanol to block endogenous peroxidases. Supplementary Table 1 details the staining procedure.

Next, non-specific binding sites were blocked by incubating with 0.25% casein/1% BSA for 30 min at room temperature. The antibodies of PD-L1 (28-8; 1:400 dilution; Abcam, Cambridge, UK), CD8 (C8/144B; 1:100 dilution; DAKO, Glostrup, Denmark), HIF1-A (EP1215Y; 1:200 dilution; Abcam, Cambridge, UK), GLUT1 (ab15309; 1:200 dilution; Abcam, Cambridge, UK), E-cadherin (HECD-1; 1:500 dilution; Takara BIO, Shiga, Japan), and Ki-67 (MIB-1; 1:40 dilution; DAKO, Glostrup, Denmark) were visualised using the HRP/DAB (Polymer) Kit (Nichirei, Tokyo, Japan) and Histofine Simple Stain MAX-PO (Multi) Kit (Nichirei) per the manufacturer's instructions. We applied the chromogen 3,3-diaminobenzidine

tetrahydrochloride (Dojindo Laboratories, Kumamoto, Japan) as a 0.02% solution containing 0.005% H₂O₂ in 50-mM Tris-HCl buffer (pH 7.6). Thereafter, the sections were lightly counterstained with Mayer's haematoxylin and mounted. Finally, we established negative controls by omitting the primary antibody.

Assessment of immunohistochemistry, TILs and ¹⁸F-FDG-uptake
We evaluated tumour cells showing membranous staining for PD-L1 as positive cells. The following semi-quantitative scoring method was used for PD-L1: 1, <1%; 2, 1–5%; 3, 6–10%; 4, 11–25%; 5, 26–50% and 6, >50% of positive cells. Notably, tumours with a score ≥ 3 were graded as high expression.²⁸ In addition, we used haematoxylin and eosin slides to assess the infiltration of TILs in the tumour stroma as recommended by the International TILs Working Group.²⁹ We assessed the percentages of the CD8 expression when compared with the total amount of nucleated cells in the stromal compartments on the basis of previous studies.³⁰ We used the median values as a cut-off point to establish bicategorical parameters (low vs high) for TILs count and CD8 expression. The median TILs and CD8 were 30% (range, 10–80%) and 20% (range, 0–60%), respectively. We considered tumour cells expressing membranous GLUT1 and nuclear HIF-1A as positive cells; they were evaluated in five fields ($\times 400$) to determine the proportion of positive cells.²² For GLUT1 and HIF-1A, we used a semi-quantitative scoring method as follows: 1, <10%; 2, 10–25%; 3, 25–50%; 4, 51–75% and 5, >75% of cells positive. We determined the positive cell score ≥ 3 as high expression of GLUT1 and HIF-1A. Moreover, E-cadherin was stained on the cell membrane as positive, for which the following scoring used a 4-point scale:³¹ 0, complete absence or negative; 1, <10% bright membrane expression; 2, $\geq 10\%$ but $\leq 50\%$ membrane expression; and 3 = >50% membrane expression. Of note, E-cadherin-positive cell score ≥ 2 was considered to be a positive expression. For Ki-67, we evaluated a highly cellular area of the immunostained sections. We defined all epithelial cells with nuclear staining of any intensity as high expression. Approximately 1000 nuclei were counted on each slide. The proliferative activity was assessed as the percentage of Ki-67-stained nuclei (Ki-67 labelling index) in the sample; the median value of the Ki-67 labelling index was 22% (range, 2–69%). Furthermore, at least two authors who were blinded to the data assessed the sections using a light microscope (Olympus Corporation, Tokyo, Japan).

In this study, the median ¹⁸F-FDG-uptake of a primary tumour was 8.85 (range, 0–37.3). ¹⁸F-FDG-uptake was compared between the cold tumour group and the others group. The median ¹⁸F-FDG-uptake of the cold tumour group was 10.98, whereas it was 6.25 in the others group. Figure 1a shows independent samples median test ($P = 0.024$). The receiver operating characteristic curve (ROC) analysis showed that the optimal cut-off value for a cold tumour was 11.4 [area under the curve (AUC), 0.65; $P = 0.04$, sensitivity, 50%, specificity, 91%; Fig. 1b]. Patients with ¹⁸F-FDG-uptake ≥ 11.4 for a cold tumour were defined as having high ¹⁸F-FDG-uptake.

PET imaging

All the patients fasted for at least 6 h before PET imaging, which was performed using a PET/CT scanner (Discovery STE; GE Healthcare, USA) with a 700-mm field of view at the Gunma University Hospital. Thereafter, we imitated three-dimensional data acquisition 50 min after intravenously injecting 5 MBq/kg of ¹⁸F-FDG. On the basis of the range of imaging, we acquired 4–10 bed positions (3-min acquisition per bed position). In addition, attenuation-corrected transverse images obtained with ¹⁸F-FDG were reconstructed with the ordered-subsets expectation maximisation algorithm into 128 \times 128 matrices with a 3.27-mm slice thickness. Two experienced nuclear physicians who were blinded to patients' clinical history and data interpreted all ¹⁸F-FDG images. Any discrepant results between the physicians were

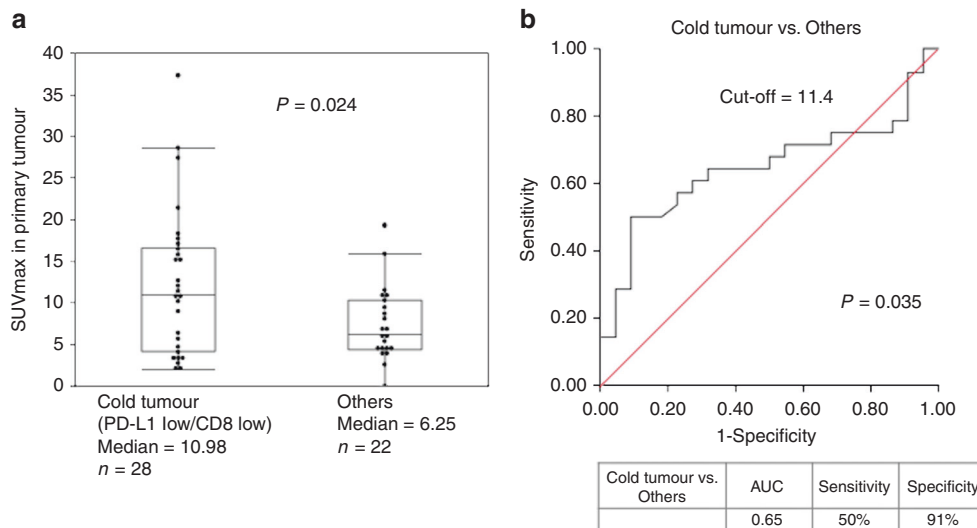


Fig. 1 The median ^{18}F -FDG-uptake of a primary tumour was 8.85 (range: 0–37.3). ^{18}F -FDG-uptake was compared between the cold tumour group and the others group. In the cold tumour group, median ^{18}F -FDG-uptake was 10.98 while it was 6.25 in the others group. **a** shows independent samples median test ($P = 0.024$). ROC analysis showed that the optimal cut-off value for a cold tumour was 11.4 (AUC = 0.65, $P = 0.04$, sensitivity = 50%, specificity = 91%; **b** Patients with ^{18}F -FDG-uptake above 11.4 for cold tumours were defined as having high ^{18}F -FDG-uptake.

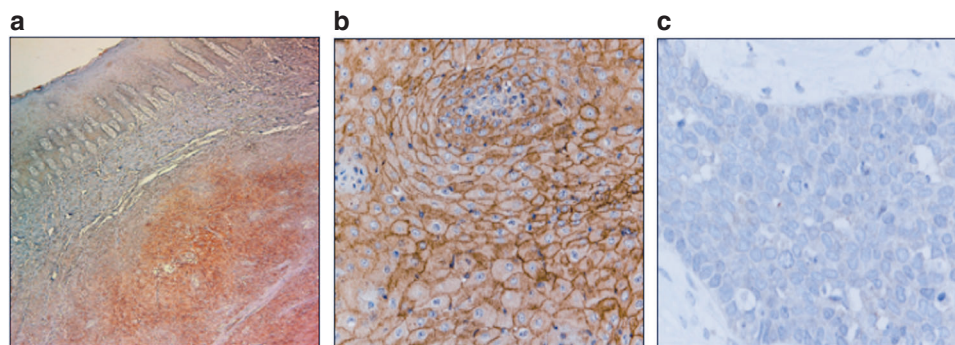


Fig. 2 The immunohistochemical analysis of the programmed death ligand-1 (PD-L1) expression in representative oral squamous cell carcinoma (OSCC) samples. **a** high PD-L1 expression in a representative OSCC tissue compared with adjacent normal oral epithelial tissue (40 \times magnification). **b** the high-power view of high PD-L1 expression in a representative OSCC tissue ($\times 200$ magnification). **c** the high-power view of low PD-L1 expression in a representative OSCC tissue ($\times 200$ magnification).

resolved by consensus. Furthermore, functional images of the standardised uptake value (SUV) were produced using attenuation-corrected transaxial images, the injected doses of ^{18}F -FDG, the patients' body weight and the cross-calibration factor between PET and the dose calibrator. We defined the SUV as follows: $\text{SUV} = \text{radioactive concentration in the region of interest (ROI)} [\text{MBq/g}] / \text{injected dose (MBq)} / \text{patient's body weight (g)}$. Of note, the ROI was manually drawn over a primary tumour on the SUV images. When a tumour was >1 cm in diameter or its shape was irregular or multifocal, an ROI of ~ 1 cm in diameter was drawn over the area corresponding to the maximal tracer uptake. A nuclear physician performed the ROI analysis using corresponding CT scans. In this study, we used the maximal SUV (SUV_{max}) in the ROI as a representative value for the assessment of ^{18}F -FDG-uptake in the primary lesion. Furthermore, we performed CT scanning for initial staging with an intravenous contrast medium, and board-certified radiologists interpreted the CT images.

Statistical analysis

In this study, statistical analyses were performed using the Mann–Whitney U-test for continuous variables, whereas the χ^2 test and analysis of variance (ANOVA) were used for categorical

variables. In addition, the Kaplan–Meier method was used to create survival curves. We used the log-rank test to assess the differences between survival curves. In addition, univariate and multivariate analyses were performed with each predictive factor using logistic regression analysis. AUC of ROC, sensitivity and specificity were calculated to detect the optimal cut-off values for ^{18}F -FDG-uptake parameters of cold tumours. We considered $P < 0.05$ to be statistically significant. JMP software version 14 (SAS Institute, Cary, NC, USA) was used to perform all statistical analyses.

RESULTS

Correlation between the PD-L1 expression and clinicopathological characteristics of OSCC

We assessed the PD-L1 expression using immunohistochemistry (IHC) in 59 OSCC samples; PD-L1 immunostaining was predominantly localised in the plasma membrane of OSCC. The PD-L1 expression levels in tumour samples were higher than those in normal samples (Fig. 2a); the representative high PD-L1 expression is shown in Fig. 2b and the representative low expression is shown in Fig. 2c. Of 59 OSCC specimens, 38

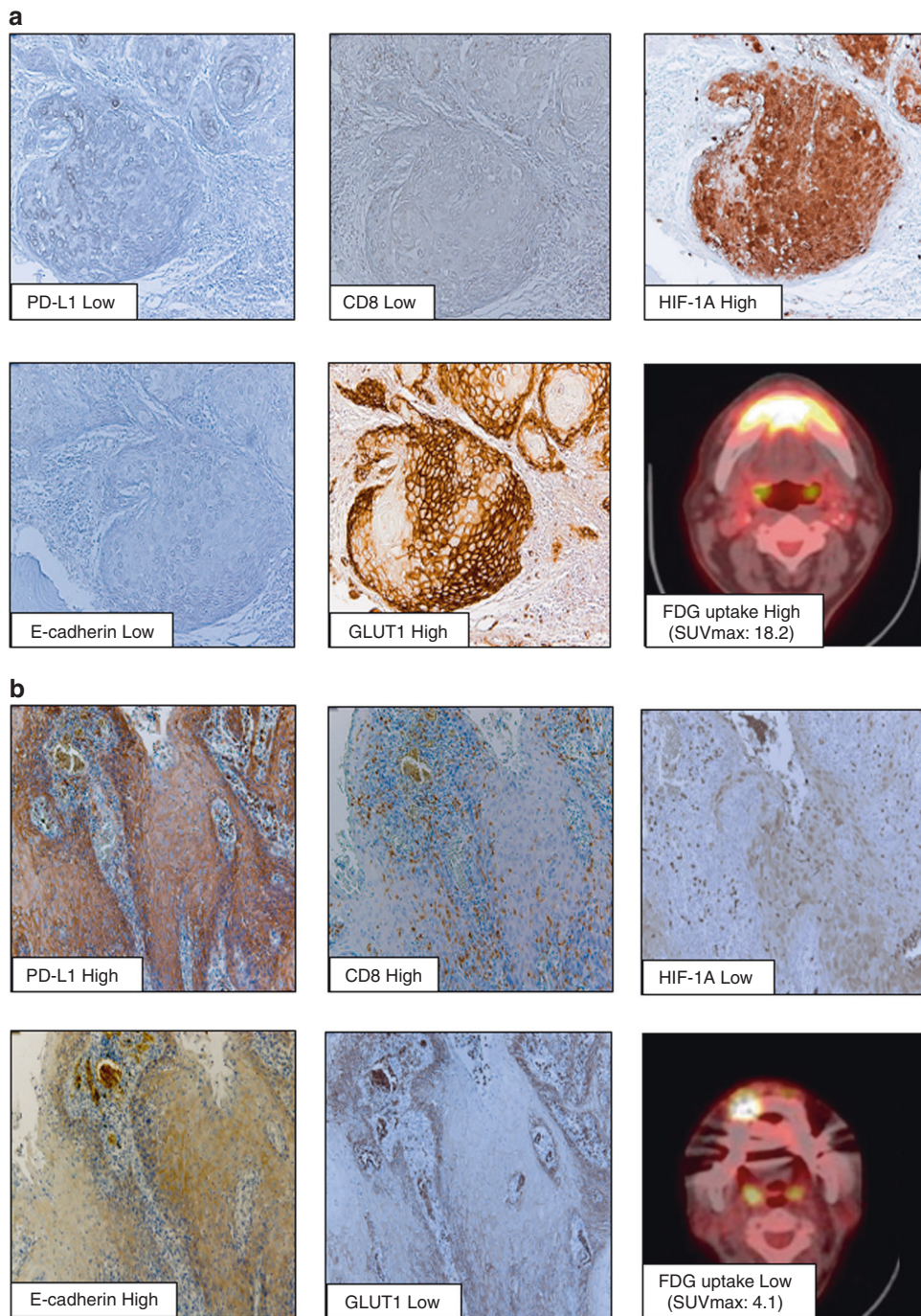


Fig. 3 Fluoro-D-glucose with positron emission tomography (FDG-PET) imaging and immunohistochemical analysis of programmed death ligand-1 (PD-L1), CD8, hypoxia-inducible factor 1 subunit alpha (HIF-1A), E-cadherin, and glucose transporter type 1 (GLUT1) in oral squamous cell carcinoma (OSCC) tissues from representative identical patients. **a** the OSCC tissue with high ^{18}F -FDG-uptake shows low expression of PD-L1 and E-cadherin, high expression of HIF-1A and GLUT1 in tumour cells and low stromal CD8, suggesting a representative cold tumour tissue ($\times 200$ magnification). **b** the OSCC tissue with low ^{18}F -FDG-uptake shows high expression of PD-L1 and E-cadherin, low expression of HIF-1A and GLUT1 in tumour cells, and high tumour stromal CD8⁺TILs, suggesting a representative hot tumour tissue ($\times 200$ magnification).

(64.4%) were assigned to the low PD-L1 expression group as PD-L1 score 1 and 2 (Fig. 3a) and 21 (35.6%) to the high PD-L1 expression group as score ≥ 3 (Fig. 3b). The percentage of PD-L1 levels with scores of 1, 2, 3, 4, 5 and 6 were 20% (12/59), 44% (26/59), 6% (4/59), 10% (6/59), 6% (4/59) and 12% (7/59), respectively. The percentages of CD8⁺TILs expression were compared with the total amount of nucleated cells in the stromal compartments. CD8⁺TILs-positive cell score $\geq 20\%$ was considered to be positive

expression. The positive expression of GLUT1 and E-cadherin was predominantly localised in the membrane, whereas that of HIF-1A and Ki-67 was localised in the nuclei. The rate of high CD8 + TILs, GLUT1 and HIF-1A was recognised in 42% (25/59), 47% (28/59) and 58% (34/59) patients, respectively. E-cadherin stained on the cell membrane was identified in 29% (17/59) patients as positive. Ki-67 was stained in the nuclei; the median value of the Ki-67 labelling index was 22% (range, 2–69%).

Table 1 presents the correlations between PD-L1 expression in OSCC specimens and clinicopathological characteristics of patients: the low PD-L1 expression group markedly correlated with the Y-K classification; tumour infiltration; high ¹⁸F-FDG-uptake; high expression of HIF-1A/GLUT1; low levels of CD8, TILs and Ki-67 and negative expression of E-cadherin (Fig. 3a) compared with those of the high PD-L1 expression group (Fig. 3b; Table 1).

In this study, we defined OSCC samples with low tumoural PD-L1 and low stromal CD8⁺TILs as cold tumours, which reportedly correlates with the low anti-tumour immune reactivity.^{15,16} Patients with a cold tumour markedly correlated with the Y-K classification, high ¹⁸F-FDG-uptake, high expression of GLUT1, low levels of TILs and negative expression of E-cadherin when compared with those of others (Table 1). Moreover, the patients with high FDG-uptake were significantly associated with the progression of tumour size, T factor, lymphatic invasion, venous invasion, stage, the high expression of HIF1-A and GLUT1 and the low expression of CD8, PD-L1 and E-cadherin compared to those with low FDG-uptake (Table 1).

Prognostic significance of the PD-L1 expression and cold tumour phenotype in patients with OSCC

Figure 4 presents the prognostic significance of PD-L1 expression and cold tumour phenotype on the overall survival. The overall survival rates of the low PD-L1 expression group ($n = 38$) were markedly worse than those of the high expression group ($n = 21$; $P = 0.007$; Fig. 4a). Furthermore, the overall survival rates of patients with OSCC with a cold tumour ($n = 34$) were markedly worse than those of other cases ($n = 25$; $P = 0.001$; Fig. 4b).

Diagnostic value of the ¹⁸F-FDG-uptake to estimate the cold tumour immune status in OSCC

In this study, we analysed the diagnostic value of clinicopathological factors for predicting the cold tumour immune status in OSCC because of the high prognostic relevance of cold tumours in patients with OSCC. Remarkably, the multivariate analysis revealed that the assessment of high ¹⁸F-FDG-uptake by non-invasive ¹⁸F-FDG-PET was an independent predictive factor for the cold tumour immune status (OR, 29.17; 95% CI, 2.79–304.2; $P = 0.005$; Table 2).

DISCUSSION

This study elucidated that the low PD-L1 expression in OSCC correlated with cancer aggressiveness, poor prognosis, high ¹⁸F-FDG-uptake with HIF-1A/GLUT1 expression, low E-cadherin expression and low CD8⁺TILs. In addition, cold tumour phenotypes as low PD-L1 tumour cells and low stromal CD8⁺TILs correlated with poor prognosis, high ¹⁸F-FDG-uptake and E-cadherin suppression. Remarkably, the assessment of high ¹⁸F-FDG-uptake using non-invasive ¹⁸F-FDG-PET scanning was an independent predictor of the cold tumour phenotype in OSCC.

Reportedly, the expression of PD-L1, which belongs to the B7/CD28 superfamily, is higher in cancer tissues than it is in non-cancerous tissues³² and cancer tissues with high PD-L1 expression correlate with cancer aggressiveness and poor prognosis.^{33,34} Conversely, some other studies have reported the opposite correlation between prognosis and PD-L1 expression in cancer tissues, including OSCC and lung SCC,³⁵ highlighting the debatable expression significance of PD-L1 in SCC tissues. This study validated the prognostic significance of low PD-L1 expression in OSCC as a poor prognostic factor. In addition, low PD-L1 expression in tumour cells correlated with high HIF-1A expression and low E-cadherin expression. Polyak and Weinberg reported that the suppression of the epithelial marker, E-cadherin, is a typical characteristic of EMT induction, which is a crucial regulatory mechanism of invasion and metastasis in cancer.³⁶

Remarkably, the HIF-1A accumulation causes EMT by upregulating ZEB1 and Wnt/ β -catenin,^{37,38} and EMT induction suppresses PD-L1 expression.³⁹ These studies indicated that OSCC patients with low PD-L1 expression could have a poorer prognosis than those with high PD-L1 expression through HIF-1A-induced EMT.

Lately, the tumour immune status, such as cold or hot tumours, has garnered substantial attention as a predictive biomarker and therapeutic target to enhance the ICI sensitivity.⁴⁰ Hot tumours with high PD-L1 expression and high CD8⁺TILs correlate with the high sensitivity of immune checkpoint blockades. Contrarily, cold tumours with low PD-L1 expression and low CD8⁺TILs correlate with their therapeutic resistance. Reportedly, HIF-1A-induced GLUT1 overexpression causes the accumulation of lactic acids in the tumour microenvironment, resulting in the suppression of CD8⁺TILs. Besides, PD-L1 expression is suppressed by the activation of the HIF-1A-EMT axis as mentioned above. Remarkably, both GLUT1 overexpression and EMT induction correlate with high ¹⁸F-FDG-uptake.⁴¹

In this study, we validated the positive correlations between high.

¹⁸F-FDG-uptake, high HIF-1A/GLUT1/EMT and cold tumour immune status in patients with OSCC. The high expression levels of PD-L1 in cancer tissues has been previously reported to be related to high ¹⁸F-FDG-uptake in several cancer patients, contrary to our OSCC data.^{20,21} As mentioned above, it has been reported that the PD-L1 expression is positively regulated by HIF-1A activation and that HIF-1A-induced GLUT1 expression is related to high PD-L1 expression and EMT induction, which is characterised by E-cadherin suppression and cancer aggressiveness.^{42,43} Conversely, PD-L1 expression has been reported to be down-regulated by EMT induction, and the high ¹⁸F-FDG-uptake in cancer tissues is negatively related to low E-cadherin expression as one of the EMT phenotypes.²³ Interestingly, the HIF-1A/GLUT1/EMT axis has been known to regulate PD-L1 expression as well as ¹⁸F-FDG-uptake,^{22,28} however, the relationship between PD-L1 expression, FDG-uptake, and the HIF-1A/GLUT1/EMT axis in identical OSCC samples has not yet been investigated. In this study, we could clarify the significant opposite correlation of high ¹⁸F-FDG-uptake and low PD-L1 expression with respect to the activation of the HIF-1A/GLUT1/EMT axis in patients with OSCC for the first time. Although the underlying mechanism regarding PD-L1 regulation in OSCC remains unclear to date, the tumoural PD-L1 may be suppressed by the activation of the HIF-1A/GLUT1/EMT axis with regard to the high ¹⁸F-FDG-uptake in OSCC, this is in contrast to the PD-L1 regulation in other cancers, which are induced by the activation of the HIF-1A signal.⁴⁴ Thus, these findings suggest that high ¹⁸F-FDG-uptake in OSCC may be associated with low PD-L1 expression because of the difference in PD-L1 regulation mechanisms between OSCC and other cancers. Although the underlying mechanism regarding the hot or cold tumour immune status remains unclear to date, we considered OSCC tumours with high ¹⁸F-FDG-uptake to have cold tumour characteristics as low PD-L1 and low CD8⁺TILs partially by the activation of the HIF-1A/GLUT1/EMT axis.

Recent research has focused on the tumour mutation burden, interferon- γ gene signature and tumour immune status on the basis of PD-L1 expression and CD8⁺TILs as representative predictive candidates of immunotherapy.^{14,37,45} However, invasive tumour tissue sampling is warranted to analyse the protein expression and extract the DNA and RNA derived from tumour tissues. In this study, we used IHC of resected OSCC samples to assess the relationship between FDG-uptake and the tumour immune status, such as cold or hot tumour, and established that high ¹⁸F-FDG-uptake by non-invasive ¹⁸F-FDG-PET scanning markedly correlated with the progression of clinicopathological factors and cold tumour immune status regarding immunotherapy resistance. The focus now must be on understanding the genetic signatures most likely to be associated with a productive response

Table 1. The relationship of clinicopathological factors, PD-L1, cold tumour phenotype, and FDG-uptake in clinical OSCC patients.

Factors	PD-L1 expression			Cold tumour ^a vs others			FDG-uptake		
	Low <i>n</i> = 38	High <i>n</i> = 21	<i>P</i> -value	Cold tumours <i>n</i> = 34	Others <i>n</i> = 25	<i>P</i> -value	Low <i>n</i> = 27	High <i>n</i> = 23	<i>P</i> -value
Age	69.3 ± 14.7	72.7 ± 12.2	0.321	70.3 ± 15.1	70.9 ± 12.4	0.982	72 ± 13.8	72.3 ± 9.6	0.661
Gender									
Male	21	7	0.106	19	9	0.131	12	12	0.586
Female	17	14		15	16		15	11	
Location									
Tongue	10	5	0.438	10	5	0.301	9	1	0.046
Gingiva	23	12		21	14		13	19	
Buccal mucosa	3	2		2	3		2	2	
Oral floor	1	2		1	2		2	1	
Lip	1	0		0	1		1	0	
Tumour size									
<2 cm	10	6	0.852	10	6	0.644	10	1	0.005*
≥2 cm	28	15		24	19		17	22	
Differentiation									
Well	24	15	0.305	22	17	0.767	16	18	0.304
Moderately	10	6		9	7		10	4	
Poorly	4	0		3	1		1	1	
T factor									
T1	11	6	0.885	11	6	0.598	10	1	0.018*
T2	14	7		11	10		9	10	
T3	6	5		5	6		6	5	
T4	7	3		7	3		2	7	
N factor									
Negative	33	20	0.307	30	23	0.636	25	19	0.279
Positive	5	1		4	2		2	4	
Metastasis									
Negative	38	21	0	34	25	0	27	23	0
Positive	0	0		0	0		0	0	
Lymphatic invasion									
Negative	22	17	0.073	20	19	0.168	24	8	<0.001*
Positive	16	4		14	6		3	15	
Venous invasion									
Negative	27	19	0.085	25	21	0.338	25	14	0.007*
Positive	11	2		9	4		2	9	
Y-K classification									
4CD	20	4	0.012*	18	6	0.025*	10	9	0.879
1, 2, 3	18	17		16	19		17	14	
INF									
a	3	6	0.018*	3	6	0.056	4	3	0.979
b	15	11		13	13		13	11	
c	20	4		18	6		10	9	
Stage									
I	11	6	0.448	11	6	0.151	10	1	0.004*
II	12	6		11	7		8	8	
III	5	6		3	8		7	4	
IV	10	3		9	4		2	10	
FDG-uptake									
Low	12	15	0.003*	14	20	0.002*	–		
High	20	3		14	2				
HIF1-A									
Low	11	14	0.005*	7	6	0.755	16	2	0.0002*
High	27	7		27	19		11	21	
GLUT1									
Low	14	17	0.001*	11	20	0.0003*	21	5	<0.0001*
High	24	4		23	5		6	18	

Table 1 continued

Factors	PD-L1 expression			Cold tumour ^a vs others			FDG-uptake		
	Low n = 38	High n = 21	P-value	Cold tumours n = 34	Others n = 25	P-value	Low n = 27	High n = 23	P-value
CD8									
Low	34	0	<0.0001*	–			11	17	0.019*
High	4	21					16	6	
TILs									
Low	24	7	0.028*	24	7	0.0007*	13	11	0.981
High	14	14		10	18		14	12	
E-cadherin									
Negative	33	9	0.0004*	30	12	0.007*	15	19	0.041*
Positive	5	12		4	13		12	4	
Ki-67 labeling index									
	18.25 ± 14.9	29.3 ± 12.6	0.0018*	19.1 ± 15.4	26.4 ± 13.6	0.0241*	23.6 ± 14	20 ± 14.1	0.419

Well well differentiated, *Moderately* moderately differentiated, *Poorly* poorly differentiated, *Y-K* Yamamoto-Kohama classification, *4CD* grade4C and grade4D, *INF* Infiltrative pattern.
**p* < 0.05 is considered statistically significant.
^aCold tumour, low tumoural PD-L1 and low intratumoural CD8+ T cells.

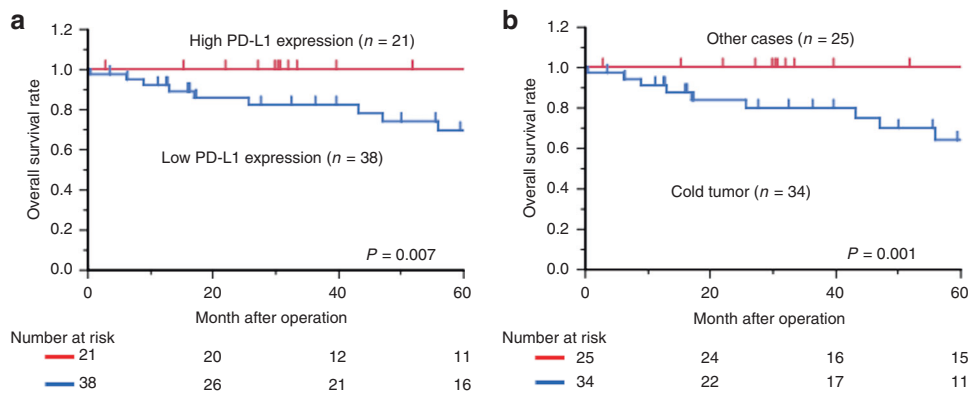


Fig. 4 Kaplan–Meier curves based on the tumour programmed death ligand-1 (PD-L1) expression and stromal CD8⁺tumour-infiltrating lymphocytes (CD8⁺TILs) in clinical oral squamous cell carcinoma (OSCC) samples. **a** the overall survival curves according to the PD-L1 expression in patients with OSCC (n = 59; P = 0.007). **b** the overall survival curves according to the cold tumour immune status as low tumour PD-L1 expression and stromal CD8⁺TILs in patients with OSCC (n = 59; P = 0.001).

to ICI therapy.⁴⁶ Thus, our data suggested that non-invasive assessment of ¹⁸F-FDG-uptake potentially identifies the micro-environment of tumours with low CD8 + TILs and low expression of PD-L1 and that the evaluation of ¹⁸F-FDG-uptake has a potential to become a crucial biomarker for determining the cancer aggressiveness and adaptation of ICI treatment in patients with OSCC in the future.

This study had some limitations. First, this was a retrospective single-institution study, and we enrolled only patients without ICIs treatment with anti-PD-1 antibodies, such as nivolumab or pembrolizumab, who had undergone surgical resection, creating an unavoidable bias. Second, the number of patients in the study was small. Recently, patients with OSCC often receive the neo-adjuvant therapy to reduce the tumour size before surgery because surgical resection of large primary tumours without neo-adjuvant therapy may cause severe and miserable cosmetic complications. Therefore, it was difficult to increase the samples number of patients with OSCC without neo-adjuvant therapy in this retrospective observational study despite our institution being identified as one of the high-volume university hospitals in Japan.

Third, the relationship between tumoural FDG-uptake and systemic inflammatory response is not examined in this study; however, Dolan RD et al., have reported that such systemic inflammatory responses influence the FDG-uptake in tumour tissues.⁴⁷ Therefore, we should analyse the relation of FDG-uptake and local tumour immune status in patients with OSCC with or without systemic inflammatory response in future studies. Finally, we did not implement any functional studies on the associations between low PD-L1, low CD8 + TILs, ¹⁸F-FDG-uptake and HIF-1A/GLUT1/EMT axis.

In conclusion, this study establishes that low PD-L1 expression in OSCC correlates with cancer progression and poor prognosis. The assessment of the PD-L1 expression level could be a biomarker of aggressive phenotypes and poor survival in patients with OSCC. In addition, high levels of ¹⁸F-FDG-uptake in OSCC markedly correlate with low PD-L1 expression and low CD8⁺TILs, suggesting the cold tumour phenotype. Overall, this study suggests that the non-invasive assessment of ¹⁸F-FDG-uptake using ¹⁸F-FDG-PET could be a promising diagnostic tool to identify cold tumours.

Table 2. Univariate and multivariate analyses of the predictive factors related to evaluation of cold tumour immune status.

Factors	Univariate analysis			Multivariate analysis		
	OR	95% CI	P-value	OR	95% CI	P-value
Age (<73/≥73) (yr.)	0.65	0.22–1.82	0.41	–	–	–
Gender (male/female)	2.25	0.78–6.50	0.13	4.71	1.18–18.7	0.03
Tumour size (<2 cm/≥2 cm)	1.31	0.4–4.28	0.65	–	–	–
T factor (T1, 2/T3, 4)	1.03	0.35–3.03	0.96	–	–	–
N factor (negative/positive)	0.65	0.11–3.88	0.64	–	–	–
Lymphatic invasion (negative/positive)	0.45	0.14–1.42	0.17	1.31	0.17–9.93	0.79
Venous invasion (negative/positive)	0.53	0.14–1.97	0.34	2.18	0.21–22.1	0.51
Y–K classification (1, 2, 3/4 C, 4D)	3.56	1.14–11.12	0.029	7.39	1.57–34.7	0.01
Levels of FDG-uptake (Low/High)	10	1.96–51.1	0.006	29.17	2.79–304.2	0.005

OR odds ratio, CI confidence interval.

ACKNOWLEDGEMENTS

We thank Mr. Futoshi Hara, Ms. Mariko Nakamura and Ms. Sawa Nagayama for their excellent assistance.

AUTHOR CONTRIBUTIONS

Conceived and designed the study: M.T., T.Y., K.S., K.S., T.O. Performed the experiments: M.T., T.H. Analysed the clinical data: K.K., T.S., M.T., T.H., S.Y. Wrote the paper: M.T., T.Y., K.S., K.S., T.O.

ADDITIONAL INFORMATION

Ethics approval and consent to participate This research conformed to the Declaration of Helsinki and was approved by the Institutional Review Board for Clinical Research at Gunma University Hospital (approval number: 2018212). Informed consent was obtained with the opt-out method.

Data availability All data generated or analysed during this study are included in this published article and its supplementary information data.

Competing interests The authors declare no competing interests.

Funding information This study was supported by Grants-in-Aid for Scientific Research from the Japan Society for the Promotion of Science (JSPS); grant numbers 18K07665 and 18H02877. The work was also supported in part by the Research Grant of the Princess Takamatsu Cancer Research Fund, Suzuken Memorial Foundation and the Pancreas Research Foundation of Japan.

Supplementary information is available for this paper at <https://doi.org/10.1038/s41416-020-0820-z>.

Publisher’s note Springer Nature remains neutral with regard to jurisdictional claims in published maps and institutional affiliations.

REFERENCES

- Franceschi, D., Gupta, R., Spiro, R. H. & Shah, J. P. Improved survival in the treatment of squamous carcinoma of the oral tongue. *Am. J. Surg.* **166**, 360–365 (1993).
- Haddad, R. I., Posner, M., Hitt, R., Cohen, E. E. W., Schulten, J., Lefebvre, J. L. et al. Induction chemotherapy in locally advanced squamous cell carcinoma of the head and neck: role, controversy, and future directions. *Ann. Oncol.* **29**, 1130–1140 (2018).
- Saloura, V., Cohen, E. E., Licitra, L., Billan, S., Dinis, J., Lisby, S. et al. An open-label single-arm, phase II trial of zalutumumab, a human monoclonal anti-EGFR antibody, in patients with platinum-refractory squamous cell carcinoma of the head and neck. *Cancer Chemother. Pharm.* **73**, 1227–1239 (2014).
- Pennock, G. K. & Chow, L. Q. The evolving role of immune checkpoint inhibitors in cancer treatment. *Oncologist* **20**, 812–822 (2015).

- La-Beck, N. M., Jean, G. W., Huynh, C., Alzghari, S. K. & Lowe, D. B. Immune checkpoint inhibitors: new insights and current place in cancer therapy. *Pharmacotherapy* **35**, 963–976 (2015).
- Eggermont, A. M. M., Blank, C. U., Mandala, M., Long, G. V., Atkinson, V., Dalle, S. et al. Adjuvant pembrolizumab versus placebo in resected stage III melanoma. *N. Engl. J. Med.* **378**, 1789–1801 (2018).
- Robert, C., Schachter, J., Long, G. V., Arance, A., Grob, J. J., Mortier, L. et al. Pembrolizumab versus ipilimumab in advanced melanoma. *N. Engl. J. Med.* **372**, 2521–2532 (2015).
- Gandhi, L., Rodriguez-Abreu, D., Gadgeel, S., Esteban, E., Felip, E., De Angelis, F. et al. Pembrolizumab plus chemotherapy in metastatic non-small-cell lung cancer. *N. Engl. J. Med.* **378**, 2078–2092 (2018).
- Paz-Ares, L., Luft, A., Vicente, D., Tafreshi, A., Gumus, M., Mazieres, J. et al. Pembrolizumab plus chemotherapy for squamous non-small-cell lung cancer. *N. Engl. J. Med.* **379**, 2040–2051 (2018).
- Ferris, R. L., Blumenschein, G. Jr., Fayette, J., Guigay, J., Colevas, A. D., Licitra, L. et al. Nivolumab for recurrent squamous-cell carcinoma of the head and neck. *N. Engl. J. Med.* **375**, 1856–1867 (2016).
- Shields, B. D., Mahmoud, F., Taylor, E. M., Byrum, S. D., Sengupta, D., Koss, B. et al. Indicators of responsiveness to immune checkpoint inhibitors. *Sci. Rep.* **7**, 807 (2017).
- Kim, M. Y., Koh, J., Kim, S., Go, H., Jeon, Y. K. & Chung, D. H. Clinicopathological analysis of PD-L1 and PD-L2 expression in pulmonary squamous cell carcinoma: Comparison with tumor-infiltrating T cells and the status of oncogenic drivers. *Lung Cancer* **88**, 24–33 (2015).
- De Meulenaere, A., Vermassen, T., Creytens, D., Aspeslagh, S., Deron, P., Duprez, F. et al. Importance of choice of materials and methods in PD-L1 and TIL assessment in oropharyngeal squamous cell carcinoma. *Histopathology* **73**, 500–509 (2018).
- Rizvi, H., Sanchez-Vega, F., La, K., Chatila, W., Jonsson, P., Halpenny, D. et al. Molecular determinants of response to anti-programmed cell death (pd)-1 and anti-programmed death-ligand 1 (PD-L1) blockade in patients with non-small-cell lung cancer profiled with targeted next-generation sequencing. *J. Clin. Oncol.* **36**, 633–641 (2018).
- Wargo, J. A., Reddy, S. M., Reuben, A. & Sharma, P. Monitoring immune responses in the tumor microenvironment. *Curr. Opin. Immunol.* **41**, 23–31 (2016).
- Gujar, S., Pol, J. G. & Kroemer, G. Heating it up: Oncolytic viruses make tumors ‘hot’ and suitable for checkpoint blockade immunotherapies. *Oncoimmunology* **7**, e1442169 (2018).
- Whiteside, T. L. Head and neck carcinoma immunotherapy: facts and hopes. *Clin. Cancer Res.* **24**, 6–13 (2018).
- Lawrence, M. S., Stojanov, P., Polak, P., Kryukov, G. V., Cibulskis, K., Sivachenko, A. et al. Mutational heterogeneity in cancer and the search for new cancer-associated genes. *Nature* **499**, 214–218 (2013).
- Long, N. M. & Smith, C. S. Causes and imaging features of false positives and false negatives on F-PET/CT in oncologic imaging. *Insights Imaging* **2**, 679–698 (2011).
- Kaira, K., Higuchi, T., Naruse, I., Arisaka, Y., Tokue, A., Altan, B. et al. Metabolic activity by (18)F-FDG-PET/CT is predictive of early response after nivolumab in previously treated NSCLC. *Eur. J. Nucl. Med. Mol. Imaging* **45**, 56–66 (2018).
- Chen, R., Zhou, X., Liu, J., Huang, G. Relationship between the expression of PD-1/PD-L1 and (18)F-FDG uptake in bladder cancer. *Eur. J. Nucl. Med. Mol. Imaging* <https://doi.org/10.1007/s00259-018-4208-8> (2019).

22. Kaira, K., Endo, M., Abe, M., Nakagawa, K., Ohde, Y., Okumura, T. et al. Biologic correlation of 2-[18F]-fluoro-2-deoxy-D-glucose uptake on positron emission tomography in thymic epithelial tumors. *J. Clin. Oncol.* **28**, 3746–3753 (2010).
23. Higashi, K., Ueda, Y., Shimasaki, M., Ishigaki, Y., Nakamura, Y., Oguchi, M. et al. High FDG uptake on PET is associated with negative cell-to-cell adhesion molecule E-cadherin expression in lung adenocarcinoma. *Ann. Nucl. Med.* **31**, 590–595 (2017).
24. Sowa, T., Menju, T., Chen-Yoshikawa, T. F., Takahashi, K., Nishikawa, S., Nakanishi, T. et al. Hypoxia-inducible factor 1 promotes chemoresistance of lung cancer by inducing carbonic anhydrase IX expression. *Cancer Med.* **6**, 288–297 (2017).
25. Smith, B. N. & Bhowmick, N. A. Role of EMT in metastasis and therapy resistance. *J. Clin. Med.* **5**, E17 (2016).
26. Nagarsheth, N., Wicha, M. S. & Zou, W. Chemokines in the cancer micro-environment and their relevance in cancer immunotherapy. *Nat. Rev. Immunol.* **9**, 559–572 (2017).
27. Yamamoto, E., Miyakawa, A. & Kohama, G. Mode of invasion and lymph node metastasis in squamous cell carcinoma of the oral cavity. *Head. Neck Surg.* **6**, 938–947 (1984).
28. Kaira, K., Shimizu, K., Kitahara, S., Yajima, T., Atsumi, J., Kosaka, T. et al. 2-Deoxy-2-[fluorine-18] fluoro-d-glucose uptake on positron emission tomography is associated with programmed death ligand-1 expression in patients with pulmonary adenocarcinoma. *Eur. J. Cancer* **101**, 181–190 (2018).
29. Salgado, R., Denkert, C., Demaria, S., Sirtaine, N., Klauschen, F., Pruner, G. et al. The evaluation of tumor-infiltrating lymphocytes (TILs) in breast cancer: recommendations by an International TILs Working Group 2014. *Ann. Oncol.* **26**, 259–271 (2015).
30. Al-Shibli, K. I., Donnem, T., Al-Saad, S., Persson, M., Bremnes, R. M. & Busund, L. T. Prognostic effect of epithelial and stromal lymphocyte infiltration in non-small cell lung cancer. *Clin. Cancer Res.* **14**, 5220–5227 (2008).
31. Gotte, M., Kersting, C., Radke, I., Kiesel, L. & Wulping, P. An expression signature of syndecan-1 (CD138), E-cadherin and c-met is associated with factors of angiogenesis and lymphangiogenesis in ductal breast carcinoma in situ. *Breast Cancer Res.* **9**, R8 (2007).
32. Zou, W., Wolchok, J. D. & Chen, L. PD-L1 (B7-H1) and PD-1 pathway blockade for cancer therapy: mechanisms, response biomarkers, and combinations. *Sci. Transl. Med.* **8**, 328rv324 (2016).
33. Gao, Q., Wang, X. Y., Qiu, S. J., Yamato, I., Sho, M., Nakajima, Y. et al. Over-expression of PD-L1 significantly associates with tumor aggressiveness and postoperative recurrence in human hepatocellular carcinoma. *Clin. Cancer Res.* **2**, 971–979 (2009).
34. Wang, Q., Liu, F. & Liu, L. Prognostic significance of PD-L1 in solid tumor: an updated meta-analysis. *Med. (Baltim.)* **5**, e6369 (2017).
35. Yang, C. Y., Lin, M. W., Chang, Y. L., Wu, C. T. & Yang, P. C. Programmed cell death-ligand 1 expression is associated with a favourable immune microenvironment and better overall survival in stage I pulmonary squamous cell carcinoma. *Eur. J. Cancer* **57**, 91–103 (2016).
36. Polyak, K. & Weinberg, R. A. Transitions between epithelial and mesenchymal states: acquisition of malignant and stem cell traits. *Nat. Rev. Cancer* **9**, 265–273 (2009).
37. Zhang, W., Shi, X., Peng, Y., Wu, M., Zhang, P., Xie, R. et al. HIF-1alpha promotes epithelial-mesenchymal transition and metastasis through direct regulation of ZEB1 in colorectal cancer. *PLoS ONE* **10**, e0129603 (2015).
38. Zhang, Q., Bai, X., Chen, W., Ma, T., Hu, Q., Liang, C. et al. Wnt/beta-catenin signaling enhances hypoxia-induced epithelial-mesenchymal transition in hepatocellular carcinoma via crosstalk with hif-1alpha signaling. *Carcinogenesis* **34**, 962–973 (2013).
39. Hirai, M., Kitahara, H., Kobayashi, Y., Kato, K., Bou-Gharios, G., Nakamura, H. et al. Regulation of PD-L1 expression in a high-grade invasive human oral squamous cell carcinoma microenvironment. *Int. J. Oncol.* **50**, 41–48 (2017).
40. Teng, M. W., Ngiow, S. F., Ribas, A. & Smyth, M. J. Classifying cancers based on T-cell infiltration and PD-L1. *Cancer Res.* **75**, 2139–2145 (2015).
41. Li, W., Wei, Z., Liu, Y., Li, H., Ren, R. & Tang, Y. Increased 18F-FDG uptake and expression of Glut1 in the EMT transformed breast cancer cells induced by TGF-beta. *Neoplasia* **57**, 234–240 (2010).
42. Koh, Y. W., Han, J. H., Park, S. Y., Yoon, D. H., Suh, C. & Huh, J. GLUT1 as a prognostic factor for classical hodgkin's lymphoma: correlation with PD-L1 and PD-L2 expression. *J. Pathol. Transl. Med.* **2**, 152–158 (2017).
43. Zuo, J., Wen, J., Lei, M., Wen, M., Li, S., Lv, X. et al. Hypoxia promotes the invasion and metastasis of laryngeal cancer cells via EMT. *Med. Oncol.* **33**, 15 (2016).
44. Chang, Y. L., Yang, C. Y., Lin, M. W., Wu, C. T. & Yang, P. C. High co-expression of PD-L1 and HIF-1alpha correlates with tumour necrosis in pulmonary pleomorphic carcinoma. *Eur. J. Cancer* **60**, 125–135 (2016).
45. Goodman, A. M., Kato, S., Bazhenova, L., Patel, S. P., Frampton, G. M., Miller, V. et al. Tumor mutational burden as an independent predictor of response to immunotherapy in diverse cancers. *Mol. Cancer Ther.* **16**, 2598–2608 (2017).
46. Ward, F. J., Dahal, L. N. & Abu-Eid, R. On the road to immunotherapy-prospects for treating head and neck cancers with checkpoint inhibitor antibodies. *Front. Immunol.* **9**, 2182 (2018).
47. Dolan, R. D., McLees, N. G., Irfan, A., McSorley, S. T., Horgan, P. G., Colville, D. et al. The relationship between tumor glucose metabolism and host systemic inflammatory responses in patients with cancer: a systematic review. *J. Nucl. Med.* **60**, 467–471 (2019).



Open Access This article is licensed under a Creative Commons Attribution 4.0 International License, which permits use, sharing, adaptation, distribution and reproduction in any medium or format, as long as you give appropriate credit to the original author(s) and the source, provide a link to the Creative Commons license, and indicate if changes were made. The images or other third party material in this article are included in the article's Creative Commons license, unless indicated otherwise in a credit line to the material. If material is not included in the article's Creative Commons license and your intended use is not permitted by statutory regulation or exceeds the permitted use, you will need to obtain permission directly from the copyright holder. To view a copy of this license, visit <http://creativecommons.org/licenses/by/4.0/>.